Essential role of the *C. elegans* Arp2/3 complex in cell migration during ventral enclosure

Mariko Sawa[1,3], Shiro Suetsugu[1,3], Asako Sugimoto[5], Hiroaki Miki[2,4], Masayuki Yamamoto[6] and Tadaomi Takenawa[1,3,*]

[1]Department of Biochemistry and [2]Cancer Genomics, Institute of Medical Science, University of Tokyo, 4-6-1 Shirokanedai, Minato-ku, Tokyo 108-8639, Japan
[3]CREST and [4]PRESTO, Japan Science and Technology Corporation (JST), Minato-ku, Tokyo 108-8639, Japan
[5]Laboratory for Developmental Genomics, RIKEN Center for Developmental Biology, Kobe, Hyogo 650-0047, Japan
[6]Department of Biophysics and Biochemistry, Graduate School of Science, University of Tokyo, Bunkyo-ku, Tokyo 113-0033, Japan
*Author for correspondence (e-mail: takenawa@ims.u-tokyo.ac.jp)

Accepted 8 January 2003
Journal of Cell Science 116, 1505-1518 © 2003 The Company of Biologists Ltd
doi:10.1242/jcs.00362

Summary

Migration of cells through the reorganization of the actin cytoskeleton is essential for morphogenesis of multicellular animals. In a cell culture system, the actin-related protein (Arp) 2/3 complex functions as a nucleation core for actin polymerization when activated by the members of the WASP (Wiskott-Aldrich syndrome protein) family. However, the regulation of cell motility in vivo remains poorly understood. Here we report that homologues of the mammalian Arp2/3 complex and N-WASP in *Caenorhabditis elegans* play an important role in hypodermal cell migration during morphogenesis, a process known as ventral enclosure. In the absence of one of any of the *C. elegans* Arp2/3 complex subunits (ARX-1, ARX-2, ARX-4, ARX-5, ARX-6 or ARX-7) or of N-WASP (WSP-1), hypodermal cell migration led by actin-rich filopodia formation is inhibited during ventral enclosure owing to the reduction of filamentous actin formation. However, there is no effect on differentiation of hypodermal cells and dorsal intercalation. Disruption of the function of ARX-1 and WSP-1 in hypodermal cells also resulted in hypodermal cell arrest during ventral enclosure, suggesting that their function is cell autonomous. WSP-1 protein activated Arp2/3-mediated actin polymerization in vitro. Consistent with these results, the Arp2/3 complex and WSP-1 colocalized at the leading edge of migrating hypodermal cells. The stable localization of WSP-1 was dependent on the presence of Arp2/3 complex, suggesting an interaction between the Arp2/3 complex and WSP-1 in vivo.

Key words: *Caenorhabditis elegans*, Arp2/3 complex, WASP family proteins, Cell migration, Ventral enclosure

Introduction

The actin-related protein (Arp) 2/3 complex polymerizes new actin filaments in response to various signals (Pollard et al., 2000; Pantaloni et al., 2001; Takenawa and Miki, 2001). It functions as a core for actin polymerization when activated by members of the Wiskott-Aldrich syndrome protein (WASP) family (Machesky et al., 1999; Rohatgi et al., 1999). Upon activation of the Arp2/3 complex, rapid actin polymerization results in the formation of branched filaments, which allow the cytoskeletal reorganization needed for formation of protrusive filopodia and lamellipodia (Blanchoin et al., 2000; Pantaloni et al., 2000; Suetsugu et al., 2001). All five members of the WASP family, including WASP (Derry et al., 1994), N-WASP (Miki et al., 1996) and WAVE1-3 (Miki et al., 1998b; Suetsugu et al., 1999), activate actin polymerization through the Arp2/3 complex. Although WASP and N-WASP function downstream of Cdc42 to induce the formation of filopodia (Symons et al., 1996; Miki et al., 1998a), WAVE functions downstream of Rac and induces formation of lamellipodia (Takenawa and Miki, 2001).

Cell migration occurs at several points during the development of multicellular organisms (Bard, 1992). Although proliferating stem cells are restricted to various regions of the body, differentiated cells with specific functions migrate to their proper location for function. However, the mechanism that drives cell migration in the development of multicellular organisms remains poorly understood. The Arp2/3 complex and WASP family proteins are the most likely candidate molecules for directly driving these processes. In *Drosophila*, the Arp2/3 complex, SCAR/WAVE and WASP proteins function in actin dynamics. *Drosophila* Arp2/3 complex and SCAR/WAVE regulate cell morphogenesis in blastomeres, CNS neurons, egg chamber and adult eyes (Hudson and Cooley, 2002; Zallen et al., 2002). *Drosophila* WASP function in *Notch*-mediated cell lineage determination (Ben-Yaacov et al., 2001). In spite of the genetic evidence presented for *Drosophila*, *C. elegans* represents an excellent model system in which to determine the function of genes in development, because, unlike *Drosophila*, cell lineage is tractable and observation of entire cells is possible. Here, we have investigated the function of the Arp2/3 complex and WASP family proteins in *C. elegans* in cell migration.

Materials and Methods

Strains

Wild-type (N2 Bristol) and *C. elegans* strain SU93 *jcIs1[ajm-1::GFP]*, JR667*wIs51[seam cell::GFP marker]*, *sem-5 (n2019* and

n2030), *hmp-1 (zu278)*, *hmp-2 (zu364)*, *hmr-1 (zu389)* and *apr-1 (zu10)* were obtained from the *Caenorhabditis* Genetics Center (University of Minnesota, St Paul, MN). The marker *jcls1[ajm-1::GFP]* is an integrated array hypodermal cell marker, and *wls51[seam cell::GFP]* is an integrated seam cell marker. Strains were cultured at 20°C on NGM plates with *Escherichia coli* OP50.

Sequence analysis

The cDNA clones corresponding to *C. elegans* Arp3 (*arx-1*), Arp2 (*arx-2*), p34Arc *(arx-4)*, p21Arc (*arx-5*), p20Arc *(arx-6)*, p16Arc (*arx-7*) and N-WASP (*wsp-1*) were kindly provided by Y. Kohara at the National Institute of Genetics, Mishima, Japan. These clones are yk170f5 for *arx-1*, yk543a12 for *arx-2*, yk277h3 for *arx-4*, yk508a3 for *arx-5*, yk393h10 for *arx-6*, yk311a10 for *arx-7*, yk184g1 (WSP isoform 1) and yk9h5 (WSP-1 isoform2) for *wsp-1*. Sequences were confirmed by Sequence kit (Amersham Pharmacia Biotech).

RNA-mediated interference (RNAi) and microinjection

For soaking RNAi, the cDNA clones for components of the Arp2/3 complex and N-WASP (described above), previously cloned into pBluescript (pBS) vector, were amplified by PCR using primers complementary to the T3 and T7 promoter sequences. The resulting PCR products were used as templates for in vitro transcription by T3 and T7 RNA polymerases (Stratagene). The resulting complementary single-stranded RNAs were combined to form double-stranded RNA (dsRNA) and extracted by phenol, phenol-chloroform and chloroform followed by precipitation with 0.3 M sodium acetate (pH 5.2) and isopropanol. The resulting dsRNA was used for RNAi and was administered by the soaking method described previously (Maeda et al., 2001). Approximately 10 μg of dsRNA was dissolved in 5 μl 1×M9 (Mg^{2+} free), 3 mM spermidine (Wako, Osaka, Japan), 0.05% gelatin and 0.12% DOTAP (Roche). L4 larvae were washed with M9 several times and placed on an NGM plate without OP50 for 1 hour. Five worms were selected and immersed in RNA solution for 24 hours and then allowed to recover by incubation at 20°C on NGM plates for 36 hours before observation.

For feeding RNAi, the *arx-1* cDNA (129-831) fragment was excised by *Sac*I/*Sal*I digestion of the yk221f3 construct and subsequently cloned into pPD129.36 (gift of A. Fire, Carnegie Institute, Washington, Baltimore). The construct was transformed into *E. coli* HT115(DE3) (obtained from CGC). After induction by IPTG, the bacterial cells were seeded on NGM plates containing 50 μg/ml ampicillin, 12.5 μg/ml tetracycline and 40 mM IPTG. L4 larvae were placed on the plates and allowed to lay eggs. As a control, L4 larvae were deposited on pPD129.36-transformed HT115(DE3).

For hypodermal cell-specific RNAi, cDNA fragments were cloned downstream of the tissue-specific promoter as described previously (Hoier et al., 2000). First, the sense and anti-sense strand of *arx-1* cDNA (20-1278) and *wsp-1* cDNA (537-1116) were amplified by PCR and cloned into pBS. The primer pairs used for the sense strand of *arx-1* cDNA were: 5′sense*Bam*HI: CGCGGATCCCGG-CATGTGTGATCGACAATGG and 3′sense*Pst*I: CCAATGCATTGG-TTCTGCAGAGTAAGAGCTCCGAAAACTGG, and for anti-sense strand: 5′anti-sense*Pst*I: AACTGCAGCGGCATGTGTGATCG-ACAATGG and 3′anti-sense*Bam*HI: CGCGGATCCAGTAA-GAGCTCCGAAAACTGG. The primer pairs for sense strand of *wsp-1* cDNA were: Ws*Spe*5′: GGACTAGTGATCCACTCCAA-CACGACAATTCG and Ws*Pst*3′: CCAATGCATTGGTTCTGCA-GGCACCGCTTCCAATCGGAGCAGATG for anti-sense strand: Ws*Pst*5′: AACTGCAGGATCCACTCCAACACGACAATTCG and Ws*Spe*3′: GGACTAGTGCACCGCTTCCAATCGGAGCAGATG. The resulting cDNA fragments cloned into pBS were subcloned by *Xba*I/*Kpn*I digestion followed by insertion into the *Nhe*I/*Kpn*I-digested plasmid pPD95.86(BamHI)-lin-26p(+), which has a *lin-26* promoter region in pPD95.86 (gift of H. Qadota and K. Kaibuchi, Nagoya University, Japan). As an expression marker, the GFP fragment of pEGFP-C1 (Invitrogen) was digested by *Nhe*I/*Kpn*I and subcloned into *Nhe*I/*Kpn*I-digested pPD95.86(BamHI)-lin-26p(+). The sense and antisense constructs of *arx-1* and *wsp-1* cDNA, cloned downstream of *lin-26* promoter, were injected along with the GFP marker in pPD95.86(BamHI)-lin-26p(+) into young adult worms. Progeny were observed by DIC and confocal microscopy (Leica). To obtain better identification of transgene-expressing embryos, embryos were stained with an anti-GFP antibody (A6455, Molecular Probes, Oregon).

For overexpression of the VCA region, the *wsp-1* VCA region (1425-1794) was fused with VENUS (Nagai et al., 2002) (gift of Dr Miyawaki, RIKEN, Wako, Japan) at the WSP-1 VCA N-terminal, and subsequently cloned into pPD95.86(BamHI)-lin-26p(+). The construct was injected into young adult worms, and the progeny were observed by DIC and confocal microscopy (Leica).

Time-lapse recordings

Wild-type gravid hermaphrodites were cut transversely and the embryos placed on a 5% agar pad in M9 solution. RNAi-treated embryos, as described above, were collected from P0 hermaphrodites within 36 hours of the recovery period following RNAi immersion. The specimen was placed on a glass slide under a coverslip, sealed with Vaseline and its development was recorded by DIC microscopy. A four-dimensional series of images of GFP expression was recorded by a Multiphoton microscope as described previously (Simske and Hardin, 2001).

Antibodies and western blotting

Antibodies for ARX-1 and ARX-7 were obtained from rabbits immunized against synthetic peptides CGPSICRYNPVFGALT and CFGHGAIMRVFSGRQRL, respectively. Antisera were purified with activated CH-sepharose 4B beads (Pharmacia). Rabbit WSP-1 antiserum was raised against amino acids 475 to 598, corresponding to the VCA region of WSP-1. The antigen was first expressed as a GST fusion protein. The GST moiety was removed by thrombin digestion, and the resulting antigen was injected into rabbits. Antiserum was purified with CNBr-sepharose beads (Pharmacia) covalently coupled to the antigen. The specificity was examined by western blotting of total worm lysates. A monoclonal antibody against actin (MAB1501) was purchased from Chemicon (California), and its specificity for *C. elegans* actin was confirmed by western blotting. For western blotting, the gravid hermaphrodites were collected in M9 solution. Embryos were collected by treating adult hermaphrodites with bleach solution (2.5% NaHypochlorite, 0.5 M NaOH). In western blotting, total lysate or embryo extracts were run on a 12.5% polyacrylamide gel, blotted and probed. Approximately the same amount of embryo extract, judged from SDS-PAGE, was applied for the analysis of WSP-1 expression. Images were analyzed with NIH Image 1.62.

Immunostaining

Gravid hermaphrodites of wild-type or RNAi-treated P0 hermaphrodites within 36 hours of recovery from RNA solution were placed on poly-L-lysine-coated slides (Sigma). A coverslip was overlaid, and pressure was applied to extrude the embryo. The slide was placed on dry ice for at least 10 minutes. Immediately after removal of the coverslip, the specimen was fixed with methanol for 5 minutes and washed three times for 10 minutes in phosphate-buffered saline (PBS) (125 mM NaCl; 16.6 mM Na_2HPO_4; 8.40 mM NaH_2PO_4) containing 0.1% Tween-20 (PBST). After blocking with PBST containing 20% fetal bovine serum (FBS) and 1% skim milk for 1 hour at room temperature under a coverslip, the specimen was incubated with a primary antibody diluted in PBST with FBS and

skim milk overnight at 4°C. Antibodies against WSP-1, ARX-1 and ARX-7 were diluted 1:500, whereas the anti-actin antibody was diluted 1:1000. Anti-LIN-26 and MH27 antibodies were diluted 1:1500. Slides were washed three times for 10 minutes in PBST and then incubated with secondary antibodies for 1 hour at room temperature. Secondary antibodies were either AlexaFluor488-conjugated anti-rabbit IgG antibody (1:500, Molecular Probes) or AlexaFluor594-conjugated anti-mouse IgG antibody (1:500, Molecular Probes). Slides were washed three times in PBST and mounted using 25 mg/ml DABCO (Sigma) in 9:1 glycerol: PBS. Detection was performed by confocal laser scanning microscope (BioRad or Leica).

For immunostaining with labeled antibodies, anti-WSP-1 and anti-ARX-1 antibodies were labeled with Alexa Fluor 546 and Alexa Fluor 633 Protein Labeling Kit (Molecular Probes), respectively. Embryos were fixed and blocked as described above, then incubated with labeled antibodies overnight at 4°C. The dilutions were 1:100 for labeled anti-WSP-1 antibody and anti-ARX-1 antibody. The specimen were washed three times for 15 minutes in PBST then mounted and detected as described above.

Phalloidin staining

Wild-type or RNAi-treated embryos were collected by cutting gravid hermaphrodites within 36 hours of recovery from RNA solution and were placed on a poly-L-Lysine-coated slide. The embryos were then treated as described previously (Williams-Masson et al., 1997). The fixed embryos were incubated with Rhodamine Phalloidin (Molecular Probes) for 1 hour at room temperature and washed three times with PBST. Embryos were mounted and viewed as described above.

Pyrene-actin assay

Pyrene-actin assay was performed as described previously (Rohatgi et al., 1999). Briefly, Pyrene-labeled actin (9% final labeling) at 2 μM was added to 100 nM purified bovine N-WASP VCA or *C. elegans* WSP-1 VCA, 60 nM purified Arp2/3 complex. Bovine N-WASP VCA and *C. elegans* WSP-1 VCA were expressed as a GST fusion protein then purified with glutathione Sepharose 4B beads (Pharmacia). Arp2/3 complex was purified as described previously (Yamaguchi et al., 2002). The fluorescence was measured using a fluorescence spectrometer (Jasco).

Results

Conservation of Arp2/3 complex subunits in *C. elegans*

The Arp2/3 complex is composed of seven subunits. The function and structure of the Arp2/3 complex is thought to be highly conserved in eukaryotes (Winter et al., 1999; Gournier et al., 2001; Robinson et al., 2001); however, functional analysis of the Arp2/3 complex in *C. elegans* has not yet been reported. Thus, we examined whether the Arp2/3 subunits are present in *C. elegans* by searching the complete *C. elegans* genome (Reboul et al., 2001; Fields et al., 1999). Candidate genes for each of the seven subunits were found, and they showed approximately 60% amino acid similarity with the homologous genes from human or *Saccharomyces cerevisiae*. These genes are Y71F9AL.16 for Arp3, K07C5.1 for Arp2, Y79H2A.6 for p41Arc, Y6D11A.1 for p34Arc, Y37D8A.1 for p21Arc, C35D10.1 for p20Arc and M01B12.3 for p16Arc. We confirmed that the cDNA sequences of six out of seven subunits (excluding Y79HA.6 for p41Arc) actually correspond to the predicted amino-acid sequences (data not shown). We named these putative subunits, as they correspond to the mammalian homologues, actin-related protein 2/3 complex (*arx*)-*1* for Arp3, *arx-2* for Arp2, *arx-3* for p41Arc, *arx-4* for p34Arc, *arx-5* for p21Arc, *arx-6* for p20Arc, and *arx-7* for p16Arc.

Essential role of Arp2/3 complex in *C. elegans* morphogenesis

Next, we investigated Arp2/3 complex function in vivo by analysis of RNAi. We examined six of the seven subunits of Arp2/3 complex by the RNAi-by-soaking method (Maeda et al., 2001; Tabara et al., 1998), and the disruption of the expression of these genes by RNAi resulted in embryonic arrest during morphogenesis, with a similar terminal phenotype. This finding is consistent with the notion that the Arp2/3 complex functions as a seven-subunit complex (Winter et al., 1999; Gournier et al., 2001; Robinson et al., 2001). Hereafter, the suppression of a given gene by RNAi will be referred to by the gene followed by (RNAi), that is, *arx-1(RNAi)*. RNAi was embryonic lethal for 100% of *arx-1(RNAi)* (*n*=211), 100% of *arx-2(RNAi)* (*n*=254), 83% of *arx-4(RNAi)* (*n*=234), 78% of *arx-5(RNAi)* (*n*=261), 88% of *arx-6(RNAi)* (*n*=285) and 87% of *arx-7(RNAi)* (*n*=296). To clarify at which point during development the Arp2/3 complex is essential, we observed RNAi-treated embryos under a DIC microscope until each embryo died.

Defects in ventral enclosure by depletion of Arp2/3 complex

During *C. elegans* morphogenesis, dynamic changes in hypodermal (external epithelial) cells occur in two distinguishable steps at approximately 300 minutes after the first cleavage. First, the two pairs of anterior contralateral hypodermal cells of the extreme ventral rows migrate toward the ventral midline by elongating filopodia until they meet and form junctions at the ventral midline. Second, eight pairs of posterior contralateral hypodermal cells are then drawn together by actin contractile forces to close and form junctions. Completion of these processes yields the basic worm shape and is called ventral enclosure (Priess and Hirsh, 1986; Raich et al., 1999; Simske and Hardin, 2001; Williams-Masson et al., 1997). At approximately 400 minutes, the embryo rotates 90° and begins elongation of the body along the anterior-posterior axis, with rearrangement of hypodermal cells and organogenesis of the pharynx and intestine (Fig. 1A). Twitching, which indicates muscle cell differentiation, is first observed at about 430 minutes.

Time-lapse observations of the lethal phenotype in embryos treated by RNAi revealed that ventral enclosure was not complete. We also observed the arrested embryos with AJM-1::GFP to visualize the shape of hypodermal cells. AJM-1 is a component of the zonula adherens at the cell-cell junction and can be used to visualize epithelial boundaries within the hypodermis during enclosure (Podbilewicz and White, 1994; Mohler et al., 1998; Koppen et al., 2001). Although alignment of hypodermal cells was observed on both the left and right sides (indicated by arrowheads in Fig. 1A-C), the hypodermal cells did not migrate, resulting in failed ventral enclosure (Fig. 1B,C). However, organogenesis, monitored with AJM-1 (Fig. 1F,G), and muscle cell differentiation, monitored by twitching, appeared to progress normally. The dying embryos exhibited

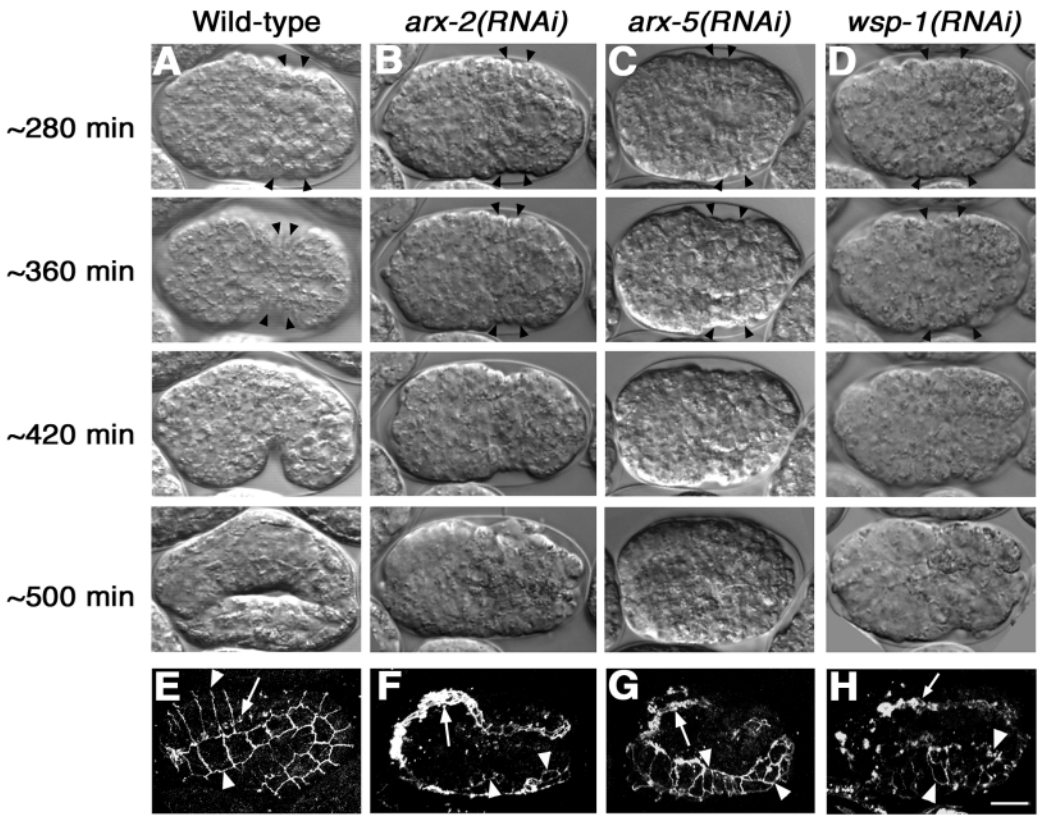

Fig. 1. *arx-2(RNAi), arx-5(RNAi)* and *wsp-1(RNAi)* show defects in morphogenesis. (A-D) Time-lapse differential interference contrast (DIC) images of wild-type (A), *arx-2(RNAi)* (B), *arx-5(RNAi)* (C) and *wsp-1(RNAi)* (D) embryos. Images were obtained at 280, 360, 420 and 500 minutes after the first cleavage. Representative hypodermal cells are indicated with arrowheads. In wild-type embryos, hypodermal cells migrated toward the ventral midline between 280 and 360 minutes. By 420 minutes, the embryo had rotated 90° and started elongation (A). These processes were not observed in RNAi-treated embryos (B-D). (E-H) Localization of adherens junction marker AJM-1 fused with GFP is shown for wild-type embryos at approximately 420 minutes (E). The terminal phenotype of *arx-2(RNAi)* (F), *arx-5(RNAi)* (G) and *wsp-1(RNAi)* (H) embryos. An arrowhead indicates a hypodermal cell, and an arrow indicates the pharynx. All embryos are shown with the anterior positioned to the left. The wild-type embryos in A at approximately 420 and 500 minutes and in E are lateral views; all other images are ventral views. Bar in H, 10 μm.

distorted hypodermal cells, suggesting that the major defects caused by depletion of Arp2/3 complex by RNAi occur in cell migration during ventral enclosure (Fig. 1E-G). We show only the results of *arx-2(RNAi)* and *arx-5(RNAi)*, but similar defects were observed with *arx-1(RNAi)*,*arx-4(RNAi)*, *arx-6(RNAi)* and *arx-7(RNAi)* (data not shown). Therefore, we conclude that the Arp2/3 complex plays an essential role in ventral enclosure in *C. elegans*.

Involvement of Arp2/3 complex in hypodermal cell migration

Previous studies have helped to identify two classes of genes involved in ventral enclosure. The first class of genes, inc*luding C*. elegans g*ex*-2 (mammalian Sra-1) and *gex-3* (mammalian HEM-2), are responsible for initiation of hypodermal cell migration. The second class of genes facilitates cell adhesion and includes genes such as *hmp-1* (α-catenin) and *hmp-2* (β-catenin) (Costa et al., 1998). Mutants of genes in this class are able to show some cell migration but either fail to form cell-cell junctions or the embryo eventually ruptures during elongation owing to weak adhesions between cells.

Analysis by DIC microscope (Fig. 1) could not completely identify the class to which the Arp2/3 complex belongs. It is possible that cells did not migrate or that cells did migrate but that the junction was not formed, resulting in dysfunctional cell-cell contacts. Therefore, we investigated whether there is a defect in cell migration during ventral enclosure in embryos depleted of Arp2/3 complex by studying the movement of epithelial cells by time-lapse observation of GFP-fused AJM-1 protein using a multiphoton microscope (Mohler et al., 1998; Mohler and White, 1998a; Mohler and White, 1998b).

The AJM-1 protein clearly indicated the boundary of migrating cells in the wild-type embryo (Simske and Hardin, 2001) (Fig. 2A). In *arx-2(RNAi)* embryos, the two pairs of anterior contralateral hypodermal cells did not migrate towards the ventral side (see cells numbered 1 and 2 in Fig. 2B). The posterior cells in *arx-2(RNAi)* embryos (including cells numbered 4 in Fig. 2B) also showed defects in migration. These arrested hypodermal cells failed to migrate, even during the period when the wild-type embryos began body elongation and organogenesis (Fig. 2B). We conclude that the abnormality in morphogenesis in *arx-2(RNAi)* embryos is caused by a defect in hypodermal cell migration not in the abnormal or incomplete formation of cell-cell junctions.

To examine the actin filament of arrested hypodermal cells, we stained RNAi-treated embryos with phalloidin. In wild-type cells, filamentous actin accumulated at the leading edge (Fig. 3A-D). By contrast, accumulation of filamentous actin was reduced in *arx-2(RNAi)* embryos arrested at ventral enclosure (Fig. 3E-H).

Differentiation of hypodermal cells in embryos depleted of Arp2/3 complex

To clarify whether or not arrested hypodermal cells had

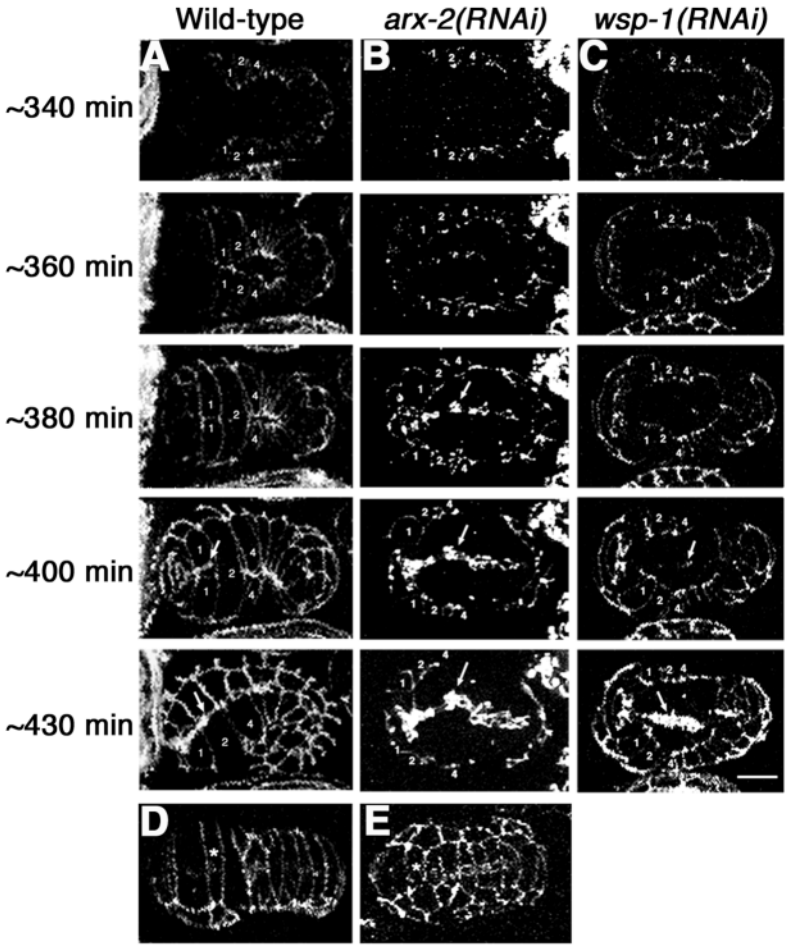

Fig. 2. *arx-2(RNAi)* and *wsp-1(RNAi)* embryos show defects in hypodermal cell migration. (A-C) Ventral view of time-lapse recording of hypodermal cell marker AJM-1 fused with GFP in wild-type (A), *arx-2(RNAi)* (B) and *wsp-1(RNAi)* (C) embryos. The 3D images of AJM-1 localization were obtained at approximately 340, 360, 380, 400 and 430 minutes after the first cleavage. Some of the contralateral pairs of hypodermal cells are numbered. The pharynx is indicated with arrows. (D,E) Dorsal view of AJM-1 expression in wild-type (D) and *arx-2(RNAi)* (E) embryos. Treatment by *arx-2(RNAi)*, which is lethal, showed normal AJM-1 expression on the dorsal side, although the width of the dorsal cells was narrowed due to the inability of the ventral cells to close (marked by asterisk). Bar, 10 μm.

differentiated, we next examined the expression of hypodermal cell differentiation markers. First, we stained RNAi-treated embryos with an anti-LIN-26 antibody. LIN-26 is a zinc-finger transcription factor that is required for hypodermal cells to acquire their proper fates (Labouesse et al., 1996). It is expressed in the nuclei among the hypodermal cells, slightly before the migration of hypodermal cells during ventral enclosure. Although the ventral hypodermal cells from *arx-1(RNAi)* embryos were defective in migration, normal LIN-26 expression was observed for these cells (Fig. 4Ad,f). Next, we analyzed the expression of a seam cell marker by a SCM::GFP fusion protein. In wild-type embryos, SCM::GFP is expressed in the nuclei of 20 seam cells after the completion of ventral enclosure. We performed RNAi on embryos expressing SCM::GFP then stained the embryos with phalloidin. The *arx-2(RNAi)* embryo showed normal expression of SCM::GFP in the all of the 20 nuclei of the seam cells (Fig. 4Bd,f). Despite junction formation failure at the ventral side during ventral enclosure, seam cells are differentiated normally. Additionally, we confirmed the normal localization of AJM-1 by observing an AJM-1::GFP fusion protein by multiphoton microscopy (Fig. 2). Slightly before ventral enclosure, the normal localization of AJM-1 of embryos with depleted Arp2/3 complexes was observed by immunostaining with an MH27 antibody, which recognizes AJM-1 (data not shown; Fig. 4Ae). Together, these results revealed that the defect in cell motility in RNAi-treated embryos was not a result of a defect occurring during differentiation.

In concert with ventral enclosure, dorsal hypodermal cells are rearranged by a process known as dorsal intercalation (Podbilewicz and White, 1994; Simske and Hardin, 2001). The zinc finger protein, DIE-1, functions in dorsal intercalation but not in ventral hypodermal cell migration (Heid et al., 2001). Some mutants, including *gex-2* (mammalian Sra-1), *gex-3* (mammalian HEM-2) (Soto et al., 2002) and *apr-1* (tumor suppressor APC related) (Hoier et al., 2000), which exhibit defects in ventral enclosure, also show defects in dorsal intercalation. However, the pattern of AJM-1 on the dorsal side was normal in *arx-2(RNAi)* embryos (Fig. 2E) as well as in embryos depleted of other Arp2/3 subunits by RNAi (data not shown). Therefore, the Arp2/3 complex does not appear to be involved in dorsal intercalation.

WASP family proteins in *C. elegans*

We then focused on the involvement of WASP family proteins in cell migration (Pollard et al., 2000; Pantaloni et al., 2001; Takenawa and Miki, 2001). In *C. elegans*, there are two WASP family proteins, WSP-1 (C07G1.4) and WVE-1 (R06C1.3), which correspond to mammalian N-WASP and WAVE, respectively. Since there are two verprolin homology (VPH) domains in C07G1.4, this gene is thought to correspond to N-WASP, which is the only WASP family protein with two VPH domains (Miki et al., 1996).

Analysis of transcripts corresponding to C07G1.4 revealed that there are two splicing variants of WSP-1 that would produce transcripts of 3.5 kb and 2.1 kb. Of 14 EST clones of C07G1.4, nine clones represented one variant (WSP-1 isoform 1) and five clones represented the other (WSP-1 isoform 2). In order to establish the existence of the splicing variants, we performed northern blot analysis on RNAs from embryos using probes against the 3′-terminal region, which is identical in both isoform 1 and 2. It revealed a major band at 2.1 kb and a minor band at 3.5 kb, suggesting that isoform 1 is the major variant (data not shown).

The open reading frame of WSP-1 isoform 1 predicts a protein of 598 amino acids (approximately 65 kDa) with high homology (approximately 50%) to mammalian N-WASP. Furthermore, the WSP-1 isoform 1 contains all of the domains found in mammalian N-WASP (Miki et al., 1996) (Fig. 5A,B), suggesting that the WSP-1 isoform 1 is the homologue of mammalian N-WASP.

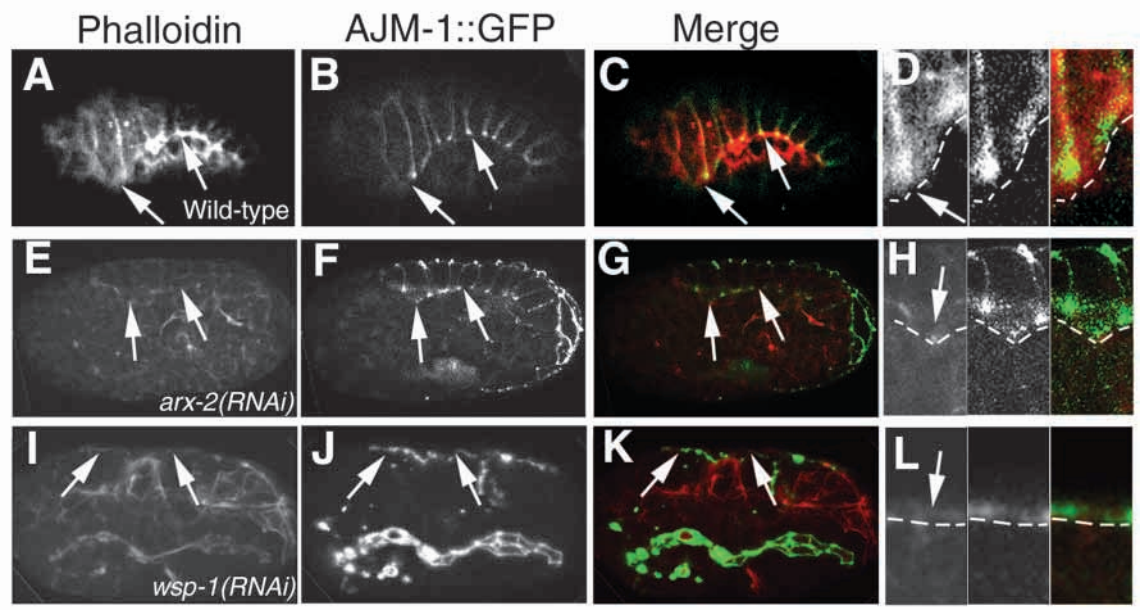

Fig. 3. Reduction of F-actin formation by *arx-2(RNAi)* and *wsp-1(RNAi)*. Phalloidin staining of embryos carrying the *jcIs1[ajm-1::GFP]*. (A-D) Wild-type, (E-H) *arx-2(RNAi)* embryo during ventral enclosure and (I-L) *wsp-1(RNAi)* embryo at the terminal phenotype. Phalloidin staining (A,E,I), expression of AJM-1::GFP (B,F,J) and merged images (C,G,K) are shown. In merged images, phalloidin staining is red, and expression of AJM-1::GFP is green. Corresponding magnified images of phalloidin (left), AJM-1GFP (center), merged image (right) are also provided (D,H,L). The leading edge is indicated with arrows (A-L) and with dotted lines (D,H,L). In the wildtype, F-actin accumulation is observed at the leading edge (A,C,D). In *arx-2(RNAi)* and *wsp-1(RNAi)* embryos, F-actin accumulation is reduced at the leading edge (E,G,H,I,K,L).

In isoform 2 of WSP-1, the N-terminal region of the WSP-1 isoform 1, including the WASP homology 1 domain and IQ motif, was replaced with amino acids with no homology to any known proteins (Fig. 5A,B). We have not, so far, determined the methionine at which the translation begins. Translation may start at either of the methionines indicated by asterisks (*1 and *2) in Fig. 5A, with a 54 kDa and a 51 kDa protein being translated from the 1*-start and 2*-start sites, respectively. If neither of these methionines is the translation start, WSP-1 isoform 2 would be more than a 70 kDa protein containing more than 660 amino acids. In all of these cases, the WSP-1 isoform 2 contains all the domains present in mammalian N-WASP except the WH1 domain and IQ motif, which suggests that isoform 2 may also form a functional interaction with Cdc42, the Arp2/3 complex, as well as SH3-domain-containing proteins such as Ash/Grb2/SEM-5.

To determine whether these WSP-1 variants are translated into proteins, we raised a specific antibody against WSP-1 using the C-terminal VCA region as the antigen. Western blot analysis of mixed stage worm cell lysates using this antibody showed only the presence of a 65 kDa protein, indicating that the majority of WSP-1 appears to be the 65 kDa isoform 1 (Fig. 5C).

WSP-1 activates Arp2/3 complex in vitro

Because the C-terminal region (VCA domain) of WASP family proteins has been shown to function as the Arp2/3-complex-activating domain in yeast and mammals, we examined the ability of the VCA domain of WSP-1 to activate Arp2/3-complex-mediated actin polymerization in vitro. In this assay,

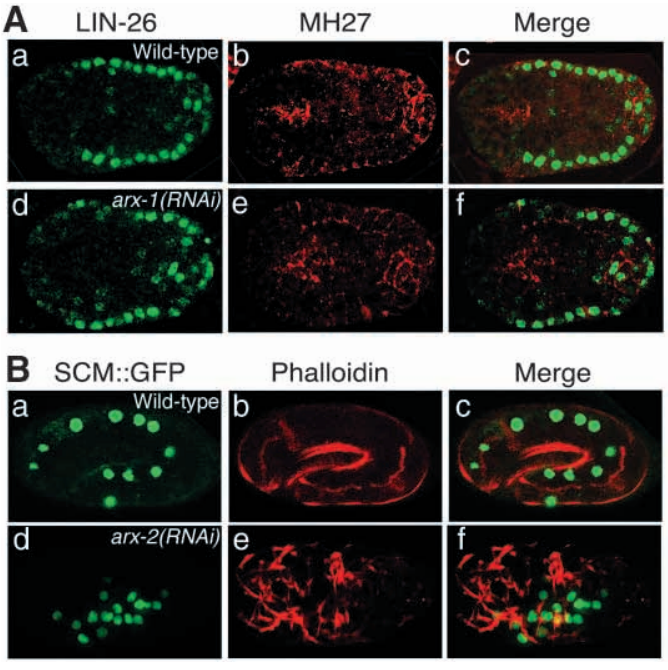

Fig. 4. Expression of the differentiation marker of hypodermal cells. (A) Immunostaining by anti-LIN-26 antibodies (a,d) and MH27 antibodies (b,e) in wild-type (a-c) and *arx-1(RNAi)* embryos (d-f). Merged images are shown in c and f. Expression of LIN-26 is green, and staining by MH27 antibody is red. (B) Phalloidin staining of embryos expressing the seam cell marker; SCM::GFP. (a-c) Wild-type. (d-f) *arx-2(RNAi)*. SCM::GFP (a,d), Phalloidin staining (b,e) and merged images (c,f) are shown. In merged images, expression of SCM::GFP is green and phalloidin staining is red.

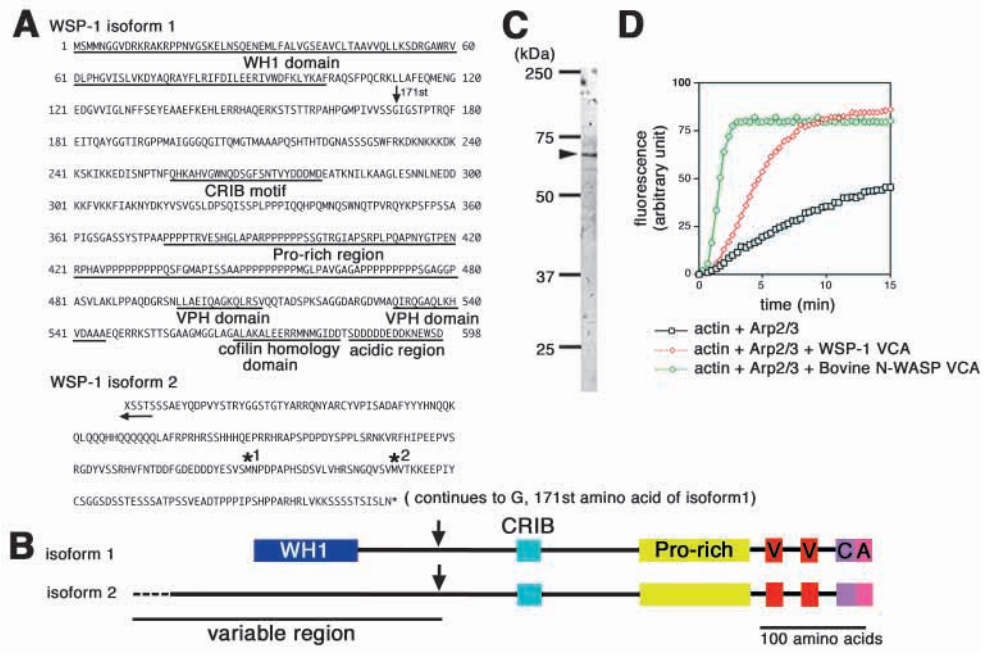

Fig. 5. Amino-acid sequence of WSP-1. (A) Amino-acid sequences of WSP-1 (*C. elegans* N-WASP) isoforms 1 and 2 are given with domains indicated by underlining. The sequence of WSP-1 isoform 2 continues to amino acid 171 of WSP-1 isoform 1. The asterisk in isoform 2 indicates the putative first methionine found in the cDNA sequence. It is possible that isoform 2 contains additional amino acids upstream of the sequence presented. (B) Domain structures of WSP-1 isoform 1 and 2. The splicing variant point is indicated with an arrowhead, and the bar indicates 100 amino acids. WH1, WASP homology 1 domain; CRIB, Cdc42/Rac interactive binding region; V, verprolin homology (VPH) domain; C, cofilin homology domain; A, acidic region. (C) Western blotting of mixed stage *C. elegans* lysates with an anti-WSP-1 antibody. A single band at 64 kDa is indicated with an arrowhead, indicating specific recognition of WSP-1 by the anti-WSP-1 antibody. (D) Activation of Arp2/3-complex-mediated actin polymerization by WSP-1. The actin polymerization assay using 60 nM bovine Arp2/3 complex and either 100 nM WSP-1 VCA or bovine N-WASP VCA. G-actin was added to a final concentration of 2 μM (9% pyrene-labeled).

bovine Arp2/3 complex was used and the activity of WSP-1 was compared to bovine N-WASP VCA, which was included as a positive control. The VCA region of WSP-1 increased Arp2/3-complex-mediated actin polymerization (Fig. 5D). Although actin polymerization mediated by WSP-1 VCA was somewhat slower than that mediated by bovine N-WASP VCA, this is probably due to differences in the specificities of bovine N-WASP and *C. elegans* WSP-1 VCA for the bovine Arp2/3 complex.

Function of WSP-1 in ventral enclosure

We investigated the in vivo role of WSP-1 in ventral enclosure by using RNAi. We synthesized dsRNA from cDNA encoding WSP-1 isoform 1 (yk184g1); however both isoforms of WSP-1 mRNA are thought to be degraded owing to the identical C-terminal region. RNAi-by-soaking with the dsRNA yielded several phenotypes: 15% were embryonic lethal, 20% showed larval arrest and 20% were sterile (n=134). Delivery of dsRNA by injection showed similar results (data not shown). In order to clarify the relationship between the Arp2/3 complex and WSP-1, we further examined the embryonic-lethal phenotype. Although the arrested embryos possessed no obvious worm shape, they did exhibit twitching, indicating muscle cell differentiation. The time-lapse series by DIC microscopy revealed incomplete ventral enclosure (Fig. 1D). AJM-1 protein localization of the terminal RNAi embryos revealed a normal pharynx and intestine; however, the distorted hypodermal cells did not cover the entire body but instead accumulated around the periphery of the embryo (Fig. 1H). We then investigated the process under a multiphoton microscope and failed to observe hypodermal migration in arrested embryos by *wsp-1(RNAi)* (Fig. 2C). We also examined

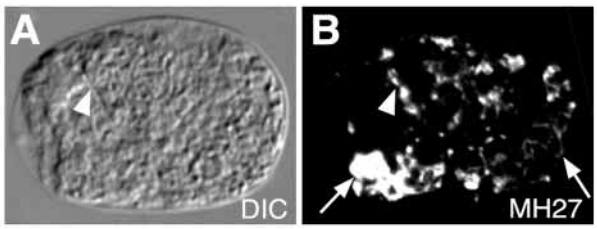

Fig. 6. Cell-specific RNAi of *arx-1* results in morphological defects. Expression of dsRNA of *arx-1* under the expression of the *lin-26* promoter caused morphological defects in embryogenesis. (A) DIC image. (B) Confocal image detecting AJM-1. The pharynx is indicated with an arrowhead; hypodermal cells are indicated with arrows.

filamentous actin formation in *wsp-1(RNAi)*-treated embryos and observed a reduction in filamentous actin formation at the edge of the hypodermal cells (Fig. 3I-L). The edge of arrested hypodermal cells (indicated with arrows) does not show filamentous actin accumulation. These phenotypes were similar to those of *arx-1(RNAi)*, *arx-2(RNAi)*, *arx-4(RNAi)*, *arx-5(RNAi)*, *arx-6(RNAi)* and *arx-7(RNAi)* embryos. The similarity in phenotypes suggests that the Arp2/3 complex and WSP-1 function in the same signaling pathway in *C. elegans*. In addition, abnormality of the dorsal side was not observed, which is again similar to that seen in embryos depleted of Arp2/3 components (data not shown). Obvious defects exhibited by the other 85% viable embryos were not related to ventral enclosure (data not shown). We also treated embryos with RNAi against both *arx-2* and *wsp-1*, but this treatment did not result in the observation of a different phenotype (n=43). Finally, distribution of the differentiation markers, LIN-26,

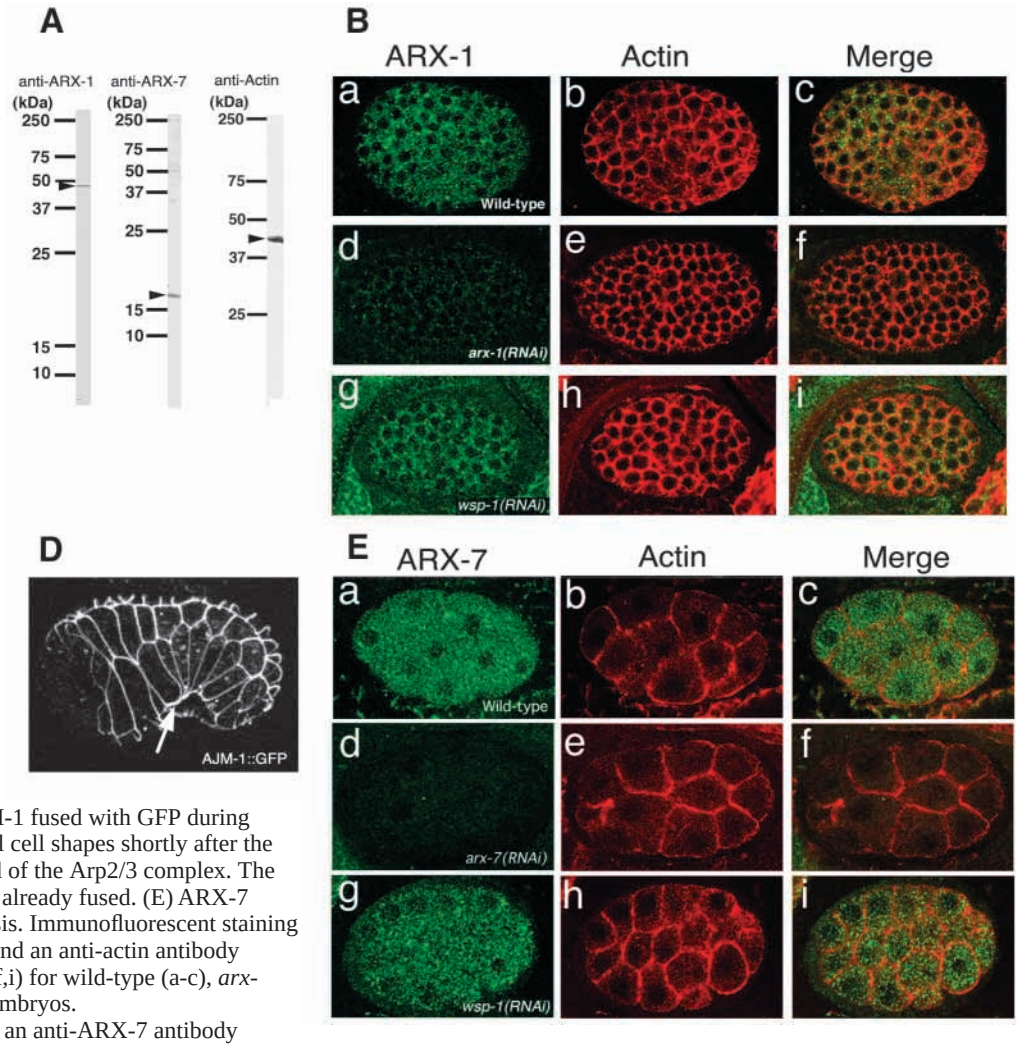

Fig. 7. Localization of the Arp2/3 complex. (A) Western blotting of total protein lysates from mixed-stage wild-type embryos with an anti-ARX-1 antibody (left), an anti-ARX-7 antibody (center) and a monoclonal antibody against actin (right). The band corresponding to each protein is indicated with an arrowhead. ARX-1 is at 48 kDa, ARX-7 is at 16 kDa and actin is at 45 kDa. (B) ARX-1 localization during early embryogenesis. Immunostaining with an anti-ARX-1 antibody (a,d,g) and an anti-actin antibody (b,e,h) with merged images shown (c,f,i) for wild-type (a-c), *arx-1(RNAi)* (d-f) and *wsp-1(RNAi)* (g-i) embryos. (C) ARX-1 localization during ventral enclosure. Immunostaining with an anti-ARX-1 antibody (a,e,i) and an anti-actin antibody (b,f,j) with merged images shown (c,g,k) for wild-type (a-d), *arx-1(RNAi)* (e-h) and *wsp-1(RNAi)* (i-l) embryos. Magnified images of hypodermal cells are shown (d,h,l) for an anti-ARX-1 antibody (left), an anti-actin antibody (center) and merged images (right). (D) Expression of AJM-1 fused with GFP during ventral enclosure showing hypodermal cell shapes shortly after the time of cell arrest in embryos depleted of the Arp2/3 complex. The two extreme anterior pairs of cells are already fused. (E) ARX-7 localization during early embryogenesis. Immunofluorescent staining with an anti-ARX-7 antibody (a,d,g) and an anti-actin antibody (b,e,h) with merged images shown (c,f,i) for wild-type (a-c), *arx-7(RNAi)* (d-f) and *wsp-1(RNAi)* (g-i) embryos. (F) Immunofluorescence staining with an anti-ARX-7 antibody (a,e,i) and an anti-actin antibody (b,f,j) and merged images (c,g,k) of wild-type (a-d), *arx-7(RNAi)* (e-h) and *wsp-1(RNAi)* (i-l) embryos. Magnified images of hypodermal cells are shown (d,h,l) for the anti-ARX-7 antibody (left), the anti-actin antibody (center) and merged images (right). In C,D,F, the anterior is positioned to the left, posterior to the right and the ventral is towards the bottom. The leading edges of the migrating hypodermal cells are indicated with arrows.

SCM::GFP and AJM-1 were not affected by *wsp-1(RNAi)* (data not shown).

Function of Arp2/3 complex and WSP-1 is cell autonomous

Previous investigations into the role of *vab-1* and *vab-2* suggested that the signaling pathway originating from the neuroblast guides hypodermal cell migration during ventral enclosure (George et al., 1998; Chin-Sang et al., 1999). By contrast, *Drosophila* WASP (*Wsp*) functions in the *Notch* signaling pathway, which suggests that WASP also functions in cell-cell signaling as well as in cell motility (Ben-Yaccov et al., 2001). Therefore, we investigated whether the Arp2/3 complex and WSP-1 function cell autonomously in hypodermal cell migration. First, we performed hypodermal cell-specific RNAi for *arx-1* and *wsp-1* by expressing sense and anti-sense RNA under the expression of the *lin-26* promoter. During embryogenesis, LIN-26 is expressed in hypodermal cells, in the deirid sheath cells and transiently in the neuroblast ALM/BDU located mid-posterior of the embryo (Labouesse et al., 1996). A plasmid, containing GFP under the expression of the *lin-26* promoter, was injected together with the RNAi constructs to monitor *lin-26*-promoter-driven expression. Although injection of the GFP marker did not result in a change of phenotype, we observed 100% embryonic lethality in embryos expressing *lin-26::arx-1* (*n*=22) and 63% in embryos expressing *lin-26::wsp-1* (*n*=11), respectively. Immunostaining with anti-ARX-1 and anti-WSP-1 antibodies revealed that ARX-1 and WSP-1 are reduced in hypodermal cells, whereas other tissues expressed ARX-1 or WSP-1 at normal levels (data not shown). Although lethal embryos exhibited the structure of a pharynx and muscle formation, they did not develop the normal worm shape (Fig. 6A,B; data not shown). These phenotypes are similar to those observed for soaking RNAi against the *Arp2/3 complex* subunits and *wsp-1*.

It has been previously been reported that overexpression of the VCA region of N-WASP has a dominant-negative effect on the Arp2/3 complex (Machesky and Insall, 1998). In order to investigate this in vivo in *C. elegans*, we expressed the VCA

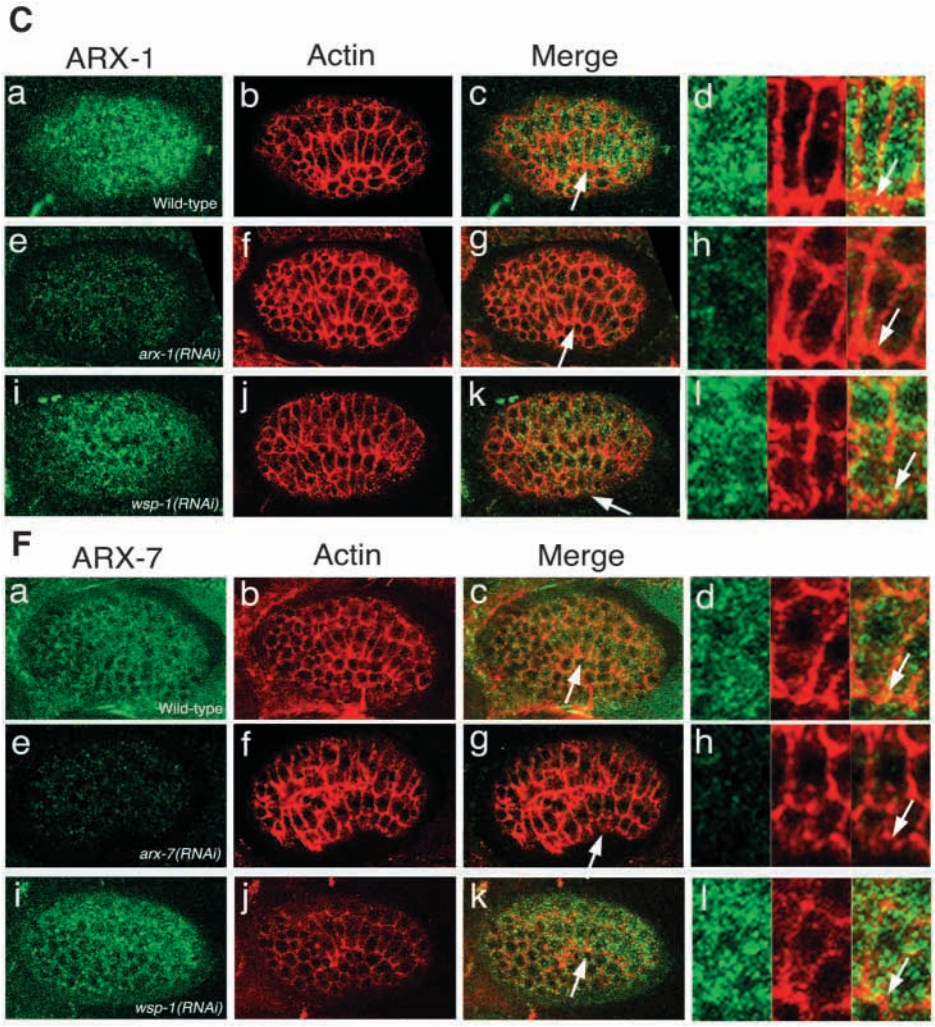

region of WSP-1 under the control of the *lin-26* promoter. Overexpression of WSP-1 VCA region resulted in embryonic lethality, with a defect in ventral enclosure. The lethal embryos showed the structure of a pharynx and were twitching, indicating muscle formation, but did not develop into a normal worm shape (data not shown). Together, these results suggest that the function of the Arp2/3 complex and WSP-1 in ventral enclosure is cell autonomous.

Localization of *C. elegans* ARX-1 and ARX-7 at hypodermal cells during ventral enclosure

We attempted to raise antibodies against ARX-1, ARX-2, ARX-5 and ARX-7. However, only antibodies against ARX-1 and ARX-7 were isolated successfully. The specificities of these antibodies were examined by western blotting mixed-staged *C. elegans* lysates. Bands at 48 kDa and 16 kDa were detected with anti-ARX-1 and anti-ARX-7 antibodies, respectively (Fig. 7A). Next, we double-stained actin and either ARX-1 or ARX-7 with their respective antibodies. During early embryogenesis, ARX-1 and ARX-7 were localized in the cytoplasm of all of the cells (Fig. 7B,E). A lateral view showing expression of these proteins in hypodermal cells during ventral enclosure in *C. elegans* embryos is shown (Fig. 7C,F). ARX-1 and ARX-7 were localized among a broad range of cells including the hypodermal cells. The similarity in localization of ARX-1 and ARX-7 supports the hypothesis that they form a complex. A reduction in the fluorescent intensities in embryos treated for both *arx-1(RNAi)* and *arx-7(RNAi)* confirmed the specificity of the staining against ARX-1 and ARX-7, respectively. In *arx-1(RNAi)* and *arx-7(RNAi)* embryos, we did not observe any obvious changes in actin localization by using an anti-actin antibody, although there was defect in actin filament formation (Fig. 3, Fig. 7Be,Cf,Ee,Ff). To determine whether WSP-1 influences localization of ARX-1 and ARX-7, we stained *wsp-1(RNAi)* embryos with anti-ARX-1 and anti-ARX-7 antibodies. However, no obvious change in the localization of the Arp2/3 complex was observed in *wsp-1(RNAi)* embryos (n>200) (Fig. 7Ci,Fi).

WSP-1 localizes at the periphery of cells

We next examined the localization of WSP-1 (Fig. 8). During early embryogenesis, WSP-1 colocalized with actin at the blastomere boundary (Fig. 8Aa-c). During ventral enclosure, WSP-1 colocalized with actin at the periphery of cells, including in hypodermal cells migrating to the ventral side (Fig. 8Aj-m), suggesting that WSP-1 functions in cell migration at cell boundaries. In *wsp-1(RNAi)* embryos, WSP-1 protein levels were reduced and localization at boundaries was diminished (Fig. 8Ad,n). Reduction of the protein level of WSP-1 was observed in almost all the RNAi-treated embryos, including those that would undergo normal embryogenesis. Anti-actin staining of *wsp-1(RNAi)* embryos did not significantly alter the actin skeleton compared to wild-type embryos (Fig. 8Ae,o).

Determination of WSP-1 localization by Arp2/3 complex

To investigate whether WSP-1 and the Arp2/3 complex interact in vivo, we first double-stained embryos expressing *ajm-1*::GFP with anti-WSP-1 antibodies conjugated to Alexa Fluor 546 and anti-ARX-1 antibodies conjugated to Alexa Fluor 633. Colocalization of WSP-1 and ARX-1 was observed at the leading edge of migrating hypodermal cells (Fig. 9). We further examined the localization of WSP-1 in embryos with disrupted Arp2/3 complexes. In 60% of *arx-5(RNAi)*-treated embryos (n=55), localization of WSP-1 at the periphery of cells was disrupted. In these embryos, WSP-1 was partially shifted to cell nuclei in blastomeres and migrating epithelial cells (data not shown). Changes in localization of WSP-1 were not only

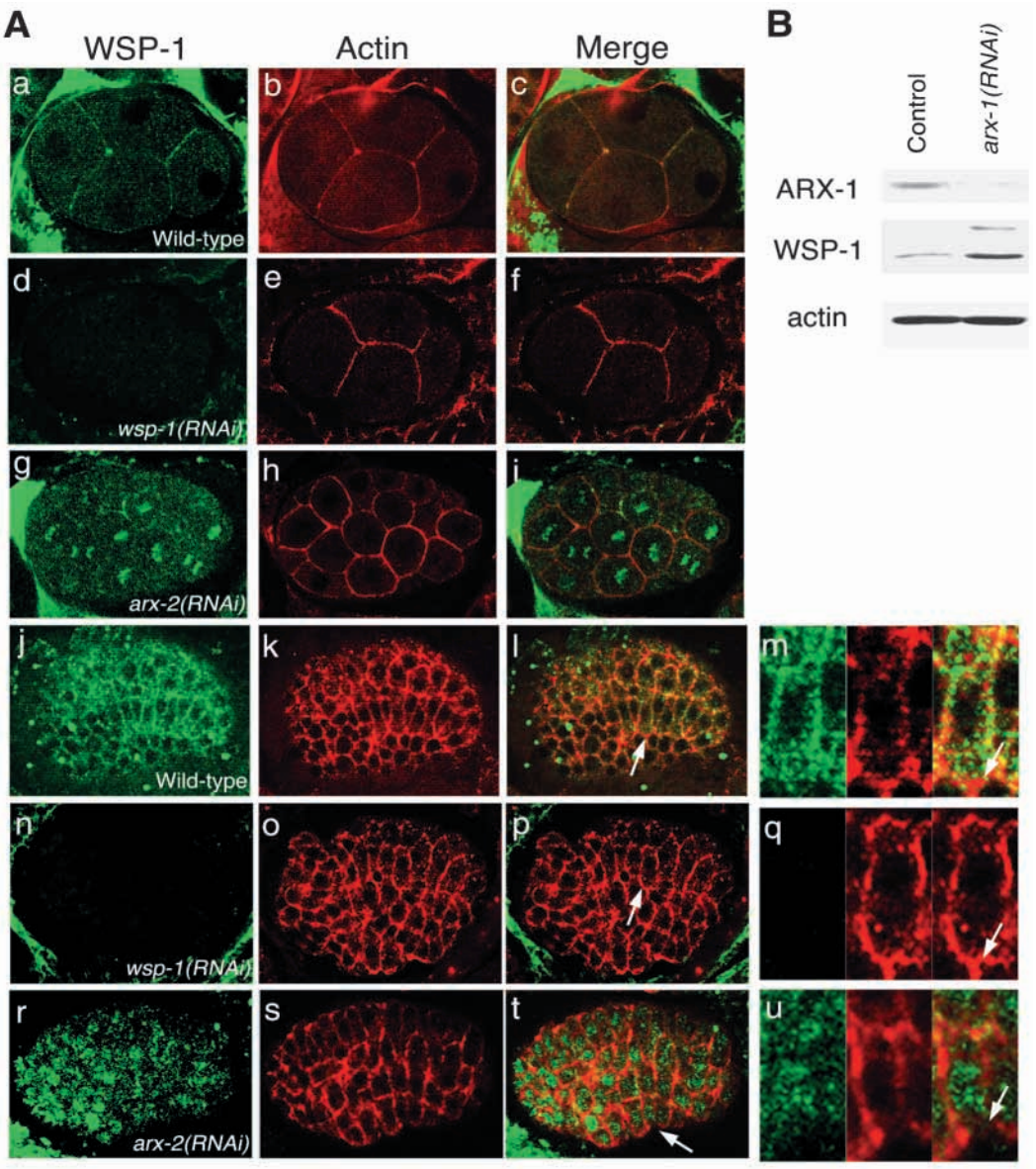

Fig. 8. WSP-1 localizes at the periphery of cells. (A) Immunostaining of WSP-1 (a,d,g,j,n,r) and actin (b,e,h,k,o,s) in wild-type (a-c,j-m), as well as *wsp-1(RNAi)* (d-f,n-q) and *arx-2(RNAi)* (g-i,r-u) treated cells. Merged images are shown in c,f,i,l,p,t. Magnified images of migrating hypodermal cells are shown (m,q,u) for the anti-WSP-1 antibody (left), the anti-actin antibody (center) and for the merged images (right). WSP-1 localizes to the periphery of cells from early development to morphogenesis (a,j). Localization of WSP-1 is partially destabilized and observed in nuclei in *arx-2(RNAi)* (g,i,r,t,u) embryos. In j-u, anterior is left, posterior is right and ventral is bottom. The leading edges of the migrating hypodermal cells are indicated with arrows. (B) Western blotting of untreated and *arx-1(RNAi)*-treated embryo lysates with an anti-ARX-1 antibody (upper lane), anti-WSP-1 antibody (middle lane) and anti-actin antibody (bottom lane). In *arx-1(RNAi)* embryos, WSP-1 isoform1 is increased by four-fold, and the upper band that corresponds with WSP-1 isoform2 was detected.

observed in *arx-5(RNAi)* but also in *arx-1(RNAi)* and *arx-2(RNAi)* embryos (Fig. 8Ag,i,r,t,u; data not shown). These findings suggest that the Arp2/3 complex is required for WSP-1 localization at the periphery of cells, including at the leading edge of migrating cells during ventral enclosure. WSP-1 and the Arp2/3 complex appear to associate and function at cell boundaries during ventral enclosure in *C. elegans*, and localization of WSP-1 is dependent on the Arp2/3 complex.

We examined the effect of molecules that regulate N-WASP on WSP-1 localization. The SH3 domain of Ash/Grb2/SEM-5 was the first N-WASP-binding partner identified (Miki et al., 1996). SEM-5, the *C. elegans* homologue of mammalian Ash/Grb2, has the conserved two SH3 domains. WSP-1 was localized at boundaries in *sem-5* (*n2019* and *n2030*) (Clark et al., 1992), mutants of *sem-5* in which one or both SH3 domains are deleted (data not shown). Cdc42 is the upstream regulator of N-WASP in mammals (Miki et al., 1998a). In the *C. elegans* embryos depleted of the Cdc42 homologue (*cdc-42(RNAi)*), WSP-1 was localized at boundaries during early cell division in common with that in wildtype (data not shown). In other mutants with ventral enclosure defects, including *apr-1* (APC-related), *hmp-1* (α-catenin), *hmp-2* (β-catenin) and *hmr-1* (cadherin), WSP-1 localization at cell boundaries was also maintained (data not shown).

Expression of WSP-1 is increased in *arx-1(RNAi)*

Next, we examined the amount of WSP-1 protein in *arx-1(RNAi)* embryos by western blotting (Fig. 8B). To harvest the embryos required for western blotting we deleted *arx-1* using RNAi by feeding. We confirmed that *arx-1(RNAi)* by feeding results in embryonic lethality (85%, *n*=294) with similar phenotypes to those observed by RNAi by soaking. The amount of ARX-1 was reduced in *arx-1(RNAi)* embryos whereas the amount of actin remained the same in control and *arx-1(RNAi)* embryos. In *arx-1(RNAi)* embryos, the anti-WSP-1 antibody recognized two bands, at approximately 65 kDa and 72 kDa, that correspond with isoform1 and 2, respectively. The intensity of the band of isoform 1 was four-fold stronger than that of the band detected in the lysate of the control embryo,

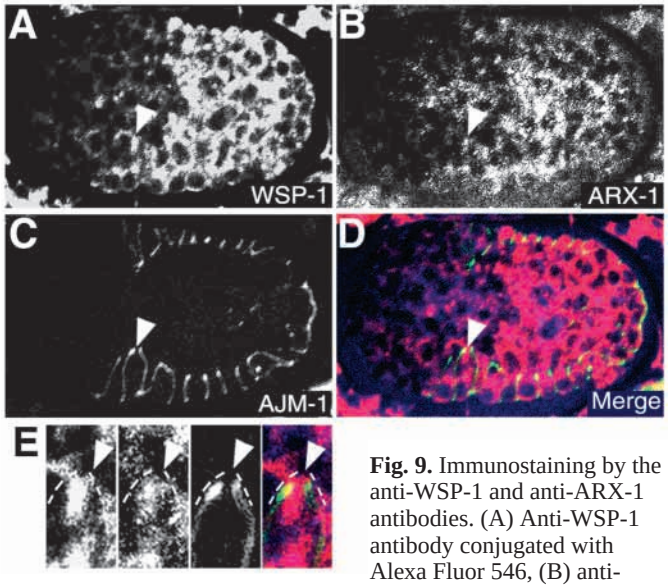

Fig. 9. Immunostaining by the anti-WSP-1 and anti-ARX-1 antibodies. (A) Anti-WSP-1 antibody conjugated with Alexa Fluor 546, (B) anti-ARX-1 antibody conjugated with Alexa Fluor 633, (C) expression of AJM-1::GFP and (D) the merged image are shown. WSP-1 is red, ARX-1 is blue and AJM-1 is green. The magnified image around the leading edge is shown in E, from left WSP-1, ARX-1, AJM-1 and the merged image. All images show the ventral view. The leading edge of the most anterior hypodermal cell is indicated with an arrowhead (A-E) and with a dotted line (E).

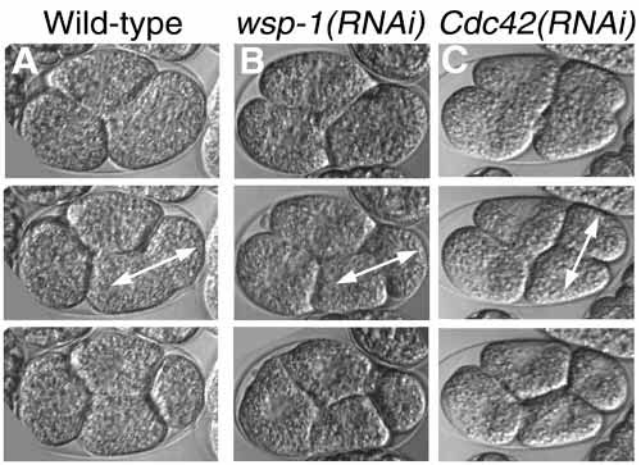

Fig. 10. Cell polarities are properly orientated in *wsp-1(RNAi)*-treated embryos. (A-C) Time-lapse recording of the three-cell to four-cell stage by DIC microscopy. The P blastomere on the right side is dividing. (A) Wild-type, (B) *wsp-1(RNAi)*- and (C) *cdc42(RNAi)*-treated embryos. In *cdc42(RNAi)* embryos, the spindle of the P blastomere is oriented longitudinally resulting in the same direction of cell division as in the AB blastomere, as reported previously (Kay and Hunter, 2001; Gotta et al., 2001). In *wsp-1(RNAi)*-treated embryos showing ventral enclosure abnormalities, normal positioning of the spindle followed by proper directional P cell division was still observed. The direction of the spindle is indicated with double-headed arrows. In A-C, the anterior is positioned to the left and the posterior to the right.

as determined by densitometry, suggesting that expression of WSP-1 is increased by the reduction of functional ARX-1.

Spindle orientation in *wsp-1(RNAi)* embryos

WSP-1 localization at cell boundaries suggests that WSP-1 functions in the formation of cell polarity. WSP-1 has a conserved Cdc42-binding motif similar to that of mammalian N-WASP and WASP. Thus, WSP-1 may function downstream of Cdc42, like PAR proteins, in the formation of cell polarity. In wild-type embryos, the one-cell embryo divides asymmetrically, producing the larger AB blastomere and the smaller P blastomere. In the second division, the spindle of the AB blastomere is oriented longitudinally, whereas it is oriented horizontally in the P blastomere (Fig. 10A). However, *cdc42(RNAi)* embryos show abnormal orientation of the spindles (Kay and Hunter, 2001; Gotta et al., 2001), such that spindles in both AB and P blastomeres are oriented horizontally (Fig. 10C). On the other hand, the *wsp-1(RNAi)* embryos did not show abnormal spindle orientation and divided asymmetrically, but later showed defects in ventral enclosure (n=7, Fig. 10B). Viable embryos did not show abnormal spindle positioning (n=43, data not shown). We also confirmed that the proper asymmetric cell division occurred even in the presence of reduced WSP-1 protein levels (Fig. 8Ad,f). Together, the results of these RNAi experiments suggest that WSP-1 does not contribute to spindle orientation during early development of *C. elegans*.

Discussion

Ventral enclosure marks the beginning of morphogenesis in *C. elegans*, with a change in embryo shape from ovoid to vermiform. This process is initiated by hypodermal cell migration and is dependent on actin polymerization. The involvement of actin filament dynamics was revealed by treatment of embryos with cytochalasin D, which inhibits actin filament formation. Cytochalasin D abolished cell migration during ventral enclosure and caused retraction of epithelial cells (Williams-Masson et al., 1997).

In the present study, we demonstrated that the Arp2/3 complex is essential for cell migration during ventral enclosure. WSP-1 functions with the Arp2/3 complex to drive cell migration, most probably by inducing actin polymerization, and these actions are likely to be cell autonomous in hypodermal cells. In addition, hypodermal cell differentiation was shown to be normal before and after ventral enclosure, indicating that WSP-1 and the Arp2/3 complex are not involved in cell differentiation. Furthermore, the Arp2/3 complex and WSP-1 seemed to form a complex at the leading edge of hypodermal cells and the results of in vitro actin polymerization assays indicate that the WSP-1-Arp2/3 pathway is likely to be conserved in *C. elegans* and mammals. On the basis of these results, we conclude that the Arp2/3 complex and WSP-1 are necessary for the actin-mediated generation of forces needed for cell migration during ventral enclosure and that these factors function cell autonomously.

During ventral enclosure, two remarkable events occur. One is hypodermal cell migration, and the other is formation of cell adhesions. In this study, we provide evidence that the *C. elegans* Arp2/3 complex and WSP-1 function in cell migration. Various strategies have been used to identify the genes involved in ventral enclosure, and cells with mutations in many of these genes show some cell migration but fail to form cell-cell

junctions, or the embryo ruptures during elongation owing to weak adhesions between cells. These mutants include *apr-1* (tumor suppressor APC related), *hmp-1* (α-catenin), *hmp-2* (β-catenin) and *hmr-1* (cadherin), all of which encode cell adhesion molecules involved in junction formation during ventral enclosure. Another gene, *mab-2* (semaphorin) (Roy et al., 2000), is needed for proper cell-cell contact, and disruption of this gene leads to embryo rupture. To date, there is little information regarding molecules involved in the initial process of hypodermal cell migration during ventral enclosure, with *gex-2* (mammalian Sra-1) or *gex-3* (mammalian HEM-2) being the lone identified genes directly involved in cell migration and dorsal intercalation during ventral enclosure (Soto et al., 2002). Mutations in these genes lead to defects in cell migration and dorsal intercalation. With the similarities in phenotypes and the possible involvement of Rho family small GTPases, which govern the signaling cascade in reorganization of actin cytoskeletons, the relationship between WSP-1, GEX-2 and GEX-3 in *C. elegans* ventral enclosure requires further study. Another class of mutants defective in ventral enclosure are *vab-1* (ephrin receptor protein-tyrosine kinase) (George et al., 1998) and *vab-2* (ephrin) (Chin-Sang et al., 1999), which function in neuroblasts. Mutation of these genes results in improperly positioned neuronal cells, which presumably disrupt a signaling pathway required for hypodermal cell migration, or the leakage of neural cells, which blocks hypodermal cell migration. Although it might be because neuronal cells are resistant to RNAi, depletion of Arp2/3 complex or *wsp-1* did not cause any defects in neural cells, which would inhibit the hypodermal cell migration.

In fact, ARX-1 and ARX-2 have high homology to actin. The cDNA sequence of *arx-2* that we used as a template for dsRNA synthesis in RNAi experiments has a region at the 3′-terminal with 90% homology to *act-2*, one of the five actin genes in *C. elegans*. Although this high homology may result in the disruption of actin, the labeling of actin was not reduced significantly in *arx-2(RNAi)* embryos (Fig. 8Ah,s). Thus, the phenotype of *arx-2(RNAi)* embryos is thought to be due solely to the disruption of ARX-2.

When RNAi against *wsp-1* was driven under the expression of the *lin-26* promoter, *lin26::wsp-1(RNAi)*, embryonic lethality was as high as 63% (n=11); soaking or injection of RNAi against *wsp-1* only yielded 15% embryonic lethality. A likely explanation is inefficient RNAi by soaking or injection. Although immunofluorescence confirmed that the levels of WSP-1 were reduced after soaking RNAi, it is possible that a small amount of WSP-1 remained beyond the limits of immunofluorescent detection. In addition, it should also be taken into account that only a small number of embryos expressing *lin26::wsp-1(RNAi)* could be detected owing to the difficulty in detecting the GFP expression marker. In this regard, it is important to consider that greater detectable GFP expression under *lin-26* promoter could reflect a greater amount of dsRNA expression, and this is the cause of the higher embryonic lethality seen for RNAi under the expression of the lin-26 promoter.

A second explanation is the existence of alternative signaling pathways that direct the Arp2/3 complex during ventral enclosure. In *lin-26::wsp-1(RNAi)*, which resulted in a high frequency of embryonic lethality, a sudden decrease of WSP-1 may not be compensated for by other proteins. WAVE (WVE-1), another WASP family member, is a candidate for regulating the Arp2/3 complex, but *wve-1(RNAi)* did not cause a detectable altered phenotype. Following double RNAi against *wsp-1* and *wve-1*, there was no increase in embryonic lethality observed (data not shown). However, we cannot conclude that WVE-1 is not involved in ventral enclosure, because the efficiency of RNAi is also dependent on the target gene.

Depletion of the Arp2/3 complex or WSP-1 did not result in arrest during early embryogenesis. During ventral enclosure, filamentous actin formation is greatly reduced by the depletion of Arp2/3 complex or WSP-1; however, actin accumulation and changes in cell shape were still observed in the ventral hypodermal cells. Immunostaining and western blotting indicated that the expression of actin did not change during RNAi against Arp2/3 complex subunits or *wsp-1*. Cultured cells injected with an antibody inhibiting the function of the Arp2/3 complex were reported to have a normal cell shape, but were unable to form lamellipodia or filopodia (Bailly et al., 2001). Furthermore, fibroblasts from N-WASP-deficient mice have normal actin cytoskeletons; however, they were defective in some types of filopodia formation (Lommel et al., 2001; Snapper et al., 2001). Together, these findings suggest that there may be other factors that regulate actin cytoskeleton reorganization independently from the Arp2/3 complex.

Although the Arp2/3 complex has been established as the nucleation core in actin polymerization, Arp2/3-complex-independent mechanisms of actin polymerization have recently been identified. Formin, a conserved Rho-GTPase effector among eukaryotes, is predicted to function in cytokinesis, polarized growth and stress fiber formation by activating actin assembly independently from the Arp2/3 complex (Evangelista et al., 2002; Pruyne et al., 2002; Sagot et al., 2002). In addition to formin, Ena/VASP regulates cell motility by binding to actin directly to promote barbed end elongation with binding to actin directly (Bear et al., 2002). Although the Arp2/3-complex-independent pathways also function in *C. elegans* from cytokinesis to morphogenesis, they may not nucleate actin as efficiently as Arp2/3-dependent pathways in dynamic reorganization of the actin cytoskeleton. Thus, defects due to disruption of Arp2/3 complex and WSP-1 might first appear at ventral enclosure with dynamic cell migration.

It is also possible that the Arp2/3 complex, WSP-1 or WVE-1 functions in other processes. Since RNAi does not represent disruption of the gene and is rather a means to inhibit gene expression, the method does not always yield complete disruption of gene expression. The nervous system, which requires cell motility during development, is resistant to RNAi (Tavernarakis et al., 2000). Furthermore, in our analysis, RNAi was performed on L4 and adult animals by soaking, feeding or microinjection of plasmid-based dsRNA under the expression of the *lin-26* promoter. Taking these considerations into account, we may not have detected all of the functions of the Arp2/3 complex, WSP-1 or WVE-1. In *Drosophila*, disruption of the Arp2/3 complex or WAVE/SCAR causes abnormalities during oogenesis. These mutants have defects in the ring canal, an actin-dependent structure that functions as a bridge for the flow of cytoplasm from the nurse cell to the oocyte (Hudson and Cooley, 2002; Zallen et al., 2002). Although *C. elegans* does not have an obvious structure corresponding to the ring canal, it is possible that Arp2/3, WSP-1 or WVE-1 in *C. elegans* may be involved in oogenesis, since maternal proteins

may ameliorate the effect of RNAi in oogenesis in our procedure. In *Drosophila*, a mutant of WASP has been isolated and characterized. In *Drosophila*, *Wsp* functions in a *Notch*-mediated signaling pathway involved in cell lineage decision, in particular in the central nervous system and mesoderm (Ben-Yaacov et al., 2001). However, we did not detect a phenotype related to cell linage decision.

By western blotting and immunostaining, we found that the expression of WSP-1 protein is affected by the expression of ARX-1 and, furthermore, stable localization of WSP-1 requires binding to the Arp2/3 complex from early cell division to morphogenesis. WSP-1 expression is enhanced when Arp2/3 complex is decreased. These results indicate that there is a feedback system inducing WSP-1 expression when the Arp2/3 complex is absent. Immunostaining results suggest an interaction between the Arp2/3 complex and WSP-1 in vivo. In mammals, activated WASP and N-WASP bind to the Arp2/3 complex, and this might indicate that WSP-1 is activated during early cell division as well as during ventral enclosure. However, it is unclear why WSP-1 localizes in cell nuclei in embryos depleted of the Arp2/3 complex, because no nuclear N-WASP-binding molecule has been reported. WSP-1 may be recruited to nuclei in concert with its increased expression. WSP-1 may function in the rearrangement of cortical actin filaments during early cell divisions, although we did not detect a phenotype associated with this period. The localization of the Arp2/3 complex in *wsp-1(RNAi)* embryos was not affected. We assume there is additional machinery that influences the localization of the Arp2/3 complex. The dependency of WSP-1 on Arp2/3 for localization, and not vice versa, raises several questions about the relationship between Arp2/3 complex and WSP-1 localization. One is that WSP-1 and the Arp2/3 complex are both contained within a huge protein complex, and the Arp2/3 complex might determine the localization of this putative complex. In this regard, it is notable that the N-WASP regulator in mammals does not affect WSP-1 localization. Although the most characterized pathway in mammals is activation of WASP by Cdc42, Cdc42 does not influence WSP-1 localization in early cell divisions of *C. elegans*. However, during ventral enclosure, *cdc42(RNAi)* strongly influenced cells to arrest during early cell divisions, and this prevented us from examining Cdc42 function at a later stage. It has been reported that *C. elegans* Cdc42 (CDC-42) localizes to the periphery of hypodermal cells during morphogenesis, and this may influence WSP-1 localization (Chen et al., 1996). Similarly, in *Drosophila*, Cdc42 is not required for regulation of *Wsp* during cell lineage determination (Tal et al., 2002). Another candidate that may activate WSP-1 is Ash/Grb2/SEM-5. Although *sem-5* mutants have been isolated in *C. elegans*, no abnormality in ventral enclosure was observed. WSP-1 localization is also normal in *sem-5* mutants (*n2019* and *n2030*), suggesting that SEM-5 is not a regulator of WSP-1 in ventral enclosure. Therefore, the regulation of the Arp2/3-WASP pathway in *C. elegans* remains unclear.

We thank the following people for providing materials used in this work: Y. Kohara for cDNA clones for the Arp2/3 complex and WSP-1, M. C. Hersko and R. H. Waterston for the mAbMH27 and M. Labouesse for the anti-LIN-26 antibody. We are also grateful to H. Qadota and K. Kaibuchi for providing pPD95.86(BamHI)-lin-26p(+), A. Fire for pPD129.36 vector and A. Miyawaki for VENUS. Some of the strains used in this work were provided by the *Caenorhabditis* Genetics Center, which is funded by the National Center for Research Resources of the National Institutes of Health.

References

Bailly, M., Ichetovkin, I., Grant, W., Zebda, N., Machesky, L. M., Segall, J. E. and Condeelis, J. (2001). The F-actin side binding activity of the Arp2/3 complex is essential for actin nucleation and lamellipod extension. *Curr. Biol.* **11**, 620-625.

Bard, J. (1992). *Morphogenesis.* Oxford: Oxford University Press.

Bear, J. E., Svitkina, T. M., Krause, M., Schafer, D. A., Loureiro, J. J., Strasser, G. A., Maly, I. V., Chaga, O. Y., Cooper, J. A., Borisy, G. G. et al. (2002). Antagonism between Ena/VASP proteins and actin filament capping regulates fibroblast motility. *Cell* **109**, 509-521.

Ben-Yaacov, S., le Borgne, R., Abramson, I., Schweisguth, F. and Schejter, E. D. (2001). *Wasp*, the *Drosophila* Wiskott-Aldrich syndrome gene homologue, is required for cell fate decisions mediated by *Notch* signaling. *J. Cell Biol.* **152**, 1-13.

Blanchoin, L., Amann, K. J., Higgs, H. N., Marchand, J. B., Kaiser, D. A. and Pollard, T. D. (2000). Direct observation of dendritic actin filament networks nucleated by Arp2/3 complex and WASP/Scar proteins. *Nature* **404**, 1007-1011.

Chen, W., Chen, S., Yap, S. F. and Lim, L. (1996). The *Caenorhabditis elegans* p21-activated kinase (CePAK) colocalizes with CeRac1 and CDC42Ce at hypodermal cell boundaries during embryo elongation. *J. Biol. Chem.* **271**, 26362-26368.

Chin-Sang, I. D., George, S. E., Ding, M., Moseley, S. L., Lynch, A. S. and Chisholm, A. D. (1999). The ephrin VAB-2/EFN-1 functions in neuronal signaling to regulate epidermal morphogenesis in *C. elegans*. *Cell* **99**, 781-790.

Clark, S. G., Stern, M. J. and Horvitz, H. R. (1992). *C. elegans* cell-signaling gene *sem-5* encodes a protein with SH2 and SH3 domains. *Nature* **356**, 340-344.

Costa, M., Raich, W., Agbunag, C., Leung, B., Hardin, J. and Priess, J. R. (1998). A putative catenin-cadherin system mediates morphogenesis of the *Caenorhabditis elegans* embryo. *J. Cell Biol.* **141**, 297-308.

Derry, J. M., Ochs, H. D. and Francke, U. (1994). Isolation of a novel gene mutated in Wiskott-Aldrich syndrome. *Cell* **78**, 635-644.

Evangelista, M., Pruyne, D., Amberg, D. C., Boone, C. and Bretscher, A. (2002). Formins direct Arp2/3-independent actin filament assembly to polarize cell growth in yeast. *Nat. Cell Biol.* **4**, 32-41.

Fields, S., Kohara, Y. and Lockhart, D. J. (1999). Functional genomics. *Proc. Natl. Acad. Sci. USA* **96**, 8825-8826.

George, S. E., Simokat, K., Hardin, J. and Chisholm, A. D. (1998). The VAB-1 Eph receptor tyrosine kinase functions in neural and epithelial morphogenesis in *C. elegans*. *Cell* **92**, 633-643.

Gotta, M., Abraham, M. C. and Ahringer, J. (2001). CDC-42 controls early cell polarity and spindle orientation in *C. elegans*. *Curr. Biol.* **11**, 482-488.

Gournier, H., Goley, E. D., Niderstrasser, H., Trinh, T. and Welch, M. D. (2001). Reconstitution of human Arp2/3 complex reveals critical roles of individual subunits in complex structure and activity. *Mol. Cell* **8**, 1041-1052.

Heid, P. J., Raich, W. B., Smith, R., Mohler, W. A., Simokat, K., Gendreau, S. B., Rothman, J. H. and Hardin, J. (2001). The zinc finger protein DIE-1 is required for late events during epithelial cell rearrangement in *C. elegans*. *Dev. Biol.* **236**, 165-180.

Hoier, E. F., Mohler, W. A., Kim, S. K. and Hajnal, A. (2000). The *Caenorhabditis elegans* APC-related gene *apr-1* is required for epithelial cell migration and Hox gene expression. *Genes Dev.* **14**, 874-886.

Hudson, A. M. and Cooley, L. (2002). A subset of dynamic actin rearrangements in *Drosophila* requires the Arp2/3 complex. *J. Cell Biol.* **156**, 677-687.

Kay, A. J. and Hunter, C. P. (2001). CDC-42 regulates PAR protein localization and function to control cellular and embryonic polarity in *C. elegans*. *Curr. Biol.* **11**, 474-481.

Koppen, M., Simske, J. S., Sims, P. A., Firestein, B. L., Hall, D. H., Radice, A. D., Rongo, C. and Hardin, J. D. (2001). Cooperative regulation of AJM-1 controls junctional integrity in *Caenorhabditis elegans* epithelia. *Nat. Cell Biol.* **3**, 983-991.

Labouesse, M., Hartwieg, E. and Horvitz, H. R. (1996). The *Caenorhabditis elegans* LIN-26 protein is required to specify and/or maintain all non-neuronal ectodermal cell fates. *Development* **122**, 2579-2588.

Lommel, S., Benesch, S., Rottner, K., Franz, T., Wehland, J. and Kuhn, R. (2001). Actin pedestal formation by enteropathogenic *Escherichia coli* and intracellular motility of *Shigella flexneri* are abolished in N-WASP-defective cells. *EMBO Rep.* **2**, 850-857.

Machesky, L. M. and Insall, R. H. (1998). Scar1 and the related Wiskott-Aldrich syndrome protein, WASP, regulate the actin cytoskeleton through the Arp2/3 complex. *Curr. Biol.* **8**, 1347-1356.

Machesky, L. M., Mullins, R. D., Higgs, H. N., Kaiser, D. A., Blanchoin, L., May, R. C., Hall, M. E. and Pollard, T. D. (1999). Scar, a WASp-related protein, activates nucleation of actin filaments by the Arp2/3 complex. *Proc. Natl. Acad. Sci. USA* **96**, 3739-3744.

Maeda, I., Kohara, Y., Yamamoto, M. and Sugimoto, A. (2001). Large-scale analysis of gene function in *Caenorhabditis elegans* by high-throughput RNAi. *Curr. Biol.* **11**, 171-176.

Miki, H., Miura, K. and Takenawa, T. (1996). N-WASP, a novel actin-depolymerizing protein, regulates the cortical cytoskeletal rearrangement in a PIP2-dependent manner downstream of tyrosine kinases. *EMBO J.* **15**, 5326-5335.

Miki, H., Sasaki, T., Takai, Y. and Takenawa, T. (1998a). Induction of filopodium formation by WASP-related actin-depolymerizing protein N-WASP. *Nature* **391**, 93-96.

Miki, H., Suetsugu, S. and Takenawa, T. (1998b). WAVE, a novel WASP-family protein involved in actin reorganization induced by Rac. *EMBO J.* **17**, 6932-6941.

Mohler, W. A. and White, J. G. (1998a). Stereo-4-D reconstruction and animation from living fluorescent specimens. *Biotechniques* **24**, 1006-1010, 1012.

Mohler, W. A. and White, J. G. (1998b). Multiphoton laser scanning microscopy for four-dimensional analysis of *C. elegans* embryonic development. *Optics Express* **3**, 325-331.

Mohler, W. A., Simske, J. S., Williams-Masson, E. M., Hardin, J. D. and White, J. G. (1998). Dynamics and ultrastructure of developmental cell fusions in the *Caenorhabditis elegans* hypodermis. *Curr. Biol.* **8**, 1087-1090.

Nagai, T., Ibata, K., Park, E. S., Kubota, M., Mikoshiba, K. and Miyawaki, A. (2002). A variant of yellow fluorescent protein with fast and efficient maturation for cell-biological applications. *Nat. Biotechnol.* **20**, 87-90.

Pantaloni, D., Boujemaa, R., Didry, D., Gounon, P. and Carlier, M. F. (2000). The Arp2/3 complex branches filament barbed ends: functional antagonism with capping proteins. *Nat. Cell. Biol.* **2**, 385-391.

Pantaloni, D., le Clainche, C. and Carlier, M. F. (2001). Mechanism of actin-based motility. *Science* **292**, 1502-1506.

Podbilewicz, B. and White, J. G. (1994). Cell fusions in the developing epithelial of *C. elegans*. *Dev. Biol.* **161**, 408-424.

Pollard, T. D., Blanchoin, L. and Mullins, R. D. (2000). Molecular mechanisms controlling actin filament dynamics in nonmuscle cells. *Annu. Rev. Biophys. Biomol. Struct.* **29**, 545-576.

Priess, J. R. and Hirsh, D. I. (1986). *Caenorhabditis elegans* morphogenesis: the role of the cytoskeleton in elongation of the embryo. *Dev. Biol.* **117**, 156-173.

Pruyne, D., Evangelista, M., Yang, C., Bi, E., Zigmond, S., Bretscher, A. and Boone, C. (2002). Role of formins in actin assembly: nucleation and barbed-end association. *Science* **297**, 612-615.

Raich, W. B., Agbunag, C. and Hardin, J. (1999). Rapid epithelial-sheet sealing in the *Caenorhabditis elegans* embryo requires cadherin-dependent filopodial priming. *Curr. Biol.* **9**, 1139-1146.

Reboul, J., Vaglio, P., Tzellas, N., Thierry-Mieg, N., Moore, T., Jackson, C., Shin-i, T., Kohara, Y., Thierry-Mieg, D., Thierry-Mieg, J. et al. (2001). Open-reading-frame sequence tags (OSTs) support the existence of at least 17,300 genes in *C. elegans*. *Nat. Genet.* **27**, 332-336.

Robinson, R. C., Turbedsky, K., Kaiser, D. A., Marchand, J. B., Higgs, H. N., Choe, S. and Pollard, T. D. (2001). Crystal structure of Arp2/3 complex. *Science* **294**, 1679-1684.

Rohatgi, R., Ma, L., Miki, H., Lopez, M., Kirchhausen, T., Takenawa, T. and Kirschner, M. W. (1999). The interaction between N-WASP and the Arp2/3 complex links Cdc42-dependent signals to actin assembly. *Cell* **97**, 221-231.

Roy, P. J., Zheng, H., Warren, C. E. and Culotti, J. G. (2000). *mab-20* encodes Semaphorin-2a and is required to prevent ectopic cell contacts during epidermal morphogenesis in *Caenorhabditis elegans*. *Development* **127**, 755-767.

Sagot, I., Klee, S. K. and Pellman, D. (2002). Yeast formins regulate cell polarity by controlling the assembly of actin cables. *Nat. Cell Biol.* **4**, 42-50.

Simske, J. S. and Hardin, J. (2001). Getting into shape: epidermal morphogenesis in *Caenorhabditis elegans* embryos. *Bioessays* **23**, 12-23.

Snapper, S. B., Takeshima, F., Anton, I., Liu, C. H., Thomas, S. M., Nguyen, D., Dudley, D., Fraser, H., Purich, D., Lopez-Ilasaca, M. et al. (2001). N-WASP deficiency reveals distinct pathways for cell surface projections and microbial actin-based motility. *Nat. Cell Biol.* **3**, 897-904.

Soto, M. C., Qadota, H., Kasuya, K., Inoue, M., Tsuboi, D., Mello, C. C. and Kaibuchi, K. (2002). The GEX-2 and GEX-3 proteins are required for tissue morphogenesis and cell migrations in *C. elegans*. *Genes Dev.* **16**, 620-632.

Suetsugu, S., Miki, H. and Takenawa, T. (1999). Identification of two human WAVE/SCAR homologues as general actin regulatory molecules which associate with Arp2/3 complex. *Biochem. Biophys. Res. Commun.* **260**, 296-302.

Suetsugu, S., Miki, H., Yamaguchi, H., Obinata, T. and Takenawa, T. (2001). Enhancement of branching efficiency by the actin filament-binding activity of N-WASP/WAVE2. *J. Cell Sci.* **114**, 4533-4542.

Symons, M., Derry, J. M., Karlak, B., Jiang, S., Lemahieu, V., Mccormick, F., Francke, U. and Abo, A. (1996). Wiskott-Aldrich syndrome protein, a novel effector for the GTPase CDC42Hs, is implicated in actin polymerization. *Cell* **84**, 723-734.

Tabara, H., Grishok, A. and Mello, C. C. (1998). RNAi in *C. elegans*: soaking in the genome sequence. *Science* **282,** 430-431.

Takenawa, T. and Miki, H. (2001). WASP and WAVE family proteins: key molecules for rapid rearrangement of cortical actin filaments and cell movement. *J. Cell Sci.* **114**, 1801-1809.

Tal, T., Vaizel-Ohayon, D. and Schejter, E. D. (2002). Conserved interactions with cytoskeletal but not signaling elements are an essential aspect of *Drosophila WASp* function. *Dev. Biol*. **243**, 260-271.

Tavernarakis, N., Wang, S. L., Dorovkov, M., Ryazanov, A. and Driscoll, M. (2000). Heritable and inducible genetic interference by double-stranded RNA encoded by transgenes. *Nat. Genet.* **24**, 180-183.

Williams-Masson, E. M., Malik, A. N. and Hardin, J. (1997). An actin-mediated two-step mechanism is required for ventral enclosure of the *C. elegans* hypodermis. *Development* **124**, 2889-2901.

Winter, D. C., Choe, E. Y. and Li, R. (1999). Genetic dissection of the budding yeast Arp2/3 complex: a comparison of the in vivo and structural roles of individual subunits. *Proc. Natl. Acad. Sci. USA* **96**, 7288-7293.

Winter, D., Lechler, T. and Li, R. (1999). Activation of the yeast Arp2/3 complex by bee1p, a WASP-family protein. *Curr. Biol.* **9**, 501-504.

Yamaguchi, H., Miki, H. and Takenawa, T. (2002). Two verprolin homology domains increase the Arp2/3 complex-mediated actin polymerization activities of N-WASP and WAVE1 C-terminal regions. *Biochem. Biophys. Res. Commun.* **297**, 214-219.

Zallen, J. A., Cohen, Y., Hudson, A. M., Cooley, L., Wieschaus, E. and Schejter, E. D. (2002). SCAR is a primary regulator of Arp2/3-dependent morphological events in *Drosophila*. *J. Cell Biol.* **156**, 689-701.